Available online at www.sciencedirect.com
SCIENCE DIRECT®
Harmful Algae 4 (2005) 553–574
HARMFUL ALGAE
www.elsevier.com/locate/hal

Effects of a *Prorocentrum minimum* bloom on light availability for and potential impacts on submersed aquatic vegetation in upper Chesapeake Bay

Charles L. Gallegos[a,*], Peter W. Bergstrom[b]

[a]*Smithsonian Environmental Research Center, P.O. Box 28, Edgewater, MD 21037, USA*
[b]*NOAA Chesapeake Bay Office, 410 Severn Ave. Suite 107A, Annapolis, MD 21403, USA*

Received 1 March 2004; received in revised form 1 June 2004; accepted 1 August 2004

Abstract

Extraordinary spring blooms of the dinoflagellate *Prorocentrum minimum* have been a recurring feature of upper Chesapeake Bay for many years. Though not thought to be toxic in Chesapeake Bay, these blooms produce extraordinarily high concentrations of chlorophyll, thereby increasing light attenuation. A particularly large event occurred in the spring of 2000. Here, we assess the impact of the spring 2000 *P. minimum* bloom on habitat quality for submerged aquatic vegetation (SAV) in the mesohaline region of Chesapeake Bay and its tributaries. We determined the light absorption and scattering spectrum of *P. minimum* on a per cell basis by analyzing inherent optical properties of natural samples from the Rhode River, Maryland, which were overwhelmingly dominated by *P. minimum*. Using these per cell properties, we constructed a model of light penetration incorporating observed cell counts of *P. minimum* to predict the impact of the bloom on other tributaries and main stem locations that experienced the bloom. Model estimates of diffuse attenuation coefficients agreed well with the limited measurements that were available. Impacts of the mahogany tide on diffuse attenuation coefficient ranged from negligible (10–30% increase above the seasonal median in the Patapsco and Magothy rivers), to a greater than six-fold increase (Potomac River). Attenuation coefficients in tributaries to the north and south of the bloom region either decreased or were unchanged relative to seasonal medians. Segments with SAV losses in 2000 were mostly the same as those that experienced the *P. minimum* bloom. Segments north and south of the bloom area mostly had SAV increases in 2000. Though all of the segments that experienced a decline in SAV area after the spring 2000 bloom showed an increase in 2002, the 2000 setback interrupted what otherwise has been a slow recovery in mid-Bay SAV, demonstrating the adverse impact of *P. minimum* blooms on SAV populations in Chesapeake Bay.

Keywords: Chesapeake Bay; Dinoflagellate bloom; Light attenuation; *Prorocentrum minimum*; Submersed aquatic vegetation

* Corresponding author. Tel.: +1 443 482-2240; fax: +1 443 482 2380.
E-mail address: gallegosc@si.edu (C.L. Gallegos).

1568-9883/$ – see front matter © 2004 Elsevier B.V. All rights reserved.
doi:10.1016/j.hal.2004.08.016

1. Introduction

There is substantial evidence that algal blooms are becoming increasingly frequent throughout the world's oceans, coastal waters, and estuaries as a function of natural and anthropogenic processes (Van Dolah, 2000; Anderson et al., 2002; Sellner et al., 2003). Some taxa produce known toxins that threaten living resources, public health, and local economies, while other non-toxic species can impact regions through biomass accumulation and subsequent stress induced through low dissolved oxygen concentrations (crab jubilees, see e.g., May, 1973) and occasionally, unique morphological features (spines, e.g., *Chaetoceros*; Rensel, 1993) that can reduce oxygen availability to aquatic animals. Mono-specific blooms can also alter food webs by effectively reducing primary production that is available to selective grazers (leading to elimination of bay scallops by brown tides in Long Island Sound, e.g., Bricelj and Lonsdale, 1997) as well as reducing light penetration with potential impacts on rooted aquatic vegetation (see below).

In the Chesapeake Bay, a typical late spring dominant member of the phytoplankton is the dinoflagellate *Prorocentrum minimum* (Pavillard) Schiller. The dinoflagellate has a unique annual recirculation that insures its return each year and potential for high biomass accumulations throughout the Bay and its tributaries, often referred to as 'mahogany tides'. Tyler and Seliger (1978) reported that the dinoflagellate is transported up-Bay in the winter in northern moving, more dense coastal ocean waters entering the Bay at the mouth and entraining *P. minimum* populations moving down-Bay in less dense, freshwater waters at the surface. As the population moves up the Bay in the winter, it can form occasional surface blooms as it is mixed into lighted shallow depths, but its major introduction into surface waters is at the northern end of the Bay's deep trough where it surfaces into light- and nutrient-rich spring freshet waters moving down the Bay. This April–May introduction usually coincides with or slightly follows the annual spring diatom maximum, resulting in *P. minimum* blooms in late spring–early summer as the population is advected southward in the less dense surface waters. It reaches the Bay mouth in the fall-winter to be entrained in northern moving waters moving back up the bay as described above. Annual spring blooms of *P. minimum* (formerly *P. mariae-lebouriae*) have been documented as early as 1970 (Tyler and Seliger, 1981) through the present time.

The 2000 *Prorocentrum* bloom was much larger spatially and temporally than in most previous years (Fig. 1, cf. http://www.cbrsp.org/cbrsp_toc_mb_chl_-page.htm). The bloom dominated the Bay and its tributaries for much of May into early June in places, with reported chlorophyll concentrations exceeding 300 mg m^{-3} (Lacouture, personal communication), cell densities exceeding 10^4 ml^{-1} (Butler, personal communication), and durations of 2–3 weeks (Gallegos and Jordan, 2002). Diurnal oxygen levels in the blooms were very high, reaching supersaturated levels on sunny days; unfortunately, nocturnal or pre-dawn DO levels are not available but oxygen demand in these blooms likely resulted in hypoxic conditions for some areas of the watershed.

Much of the habitat that is considered suitable for submerged aquatic vegetation (SAV) in Chesapeake Bay occurs in the many tributary embayments that are the result of the Bay's formation as a drowned river valley (see, e.g., Fig. VI-4 in Batiuk et al., 2000). These systems are protected from strong currents and energetic wave action, and, given suitable water quality, are shallow enough to allow the required 22% of surface irradiance (13% for tidal fresh and oligohaline segments, Carter et al., 2000) to penetrate to the bottom. However, these same characteristics make tributary embayments of Chesapeake Bay vulnerable to large phytoplankton blooms whenever sufficient nutrients are present (Loftus et al., 1972; Gallegos et al., 1997). Circulation in many tributary sub-estuaries of upper Chesapeake Bay in spring is dominated by changes in flow of the Susquehanna River, whereby sudden changes in renewal rate in sub-estuaries can occur due to rapid changes in salinity in the adjacent bay (Schubel and Pritchard, 1986). Such events have been shown to trigger extraordinary dinoflagellate blooms in the Rhode River, Maryland by a sequence of events involving pulsed injection of nitrogen into the sub-estuary, followed by relaxed water exchange as the direction of the salinity gradient reverses (Gallegos et al., 1992; Gallegos and Jordan, 2002). The chlorophyll concentrations in the tributary embayments can greatly exceed those in the adjacent bay, resulting in water clarity insufficient for the requirements of SAV (Gallegos and Jordan, 2002).

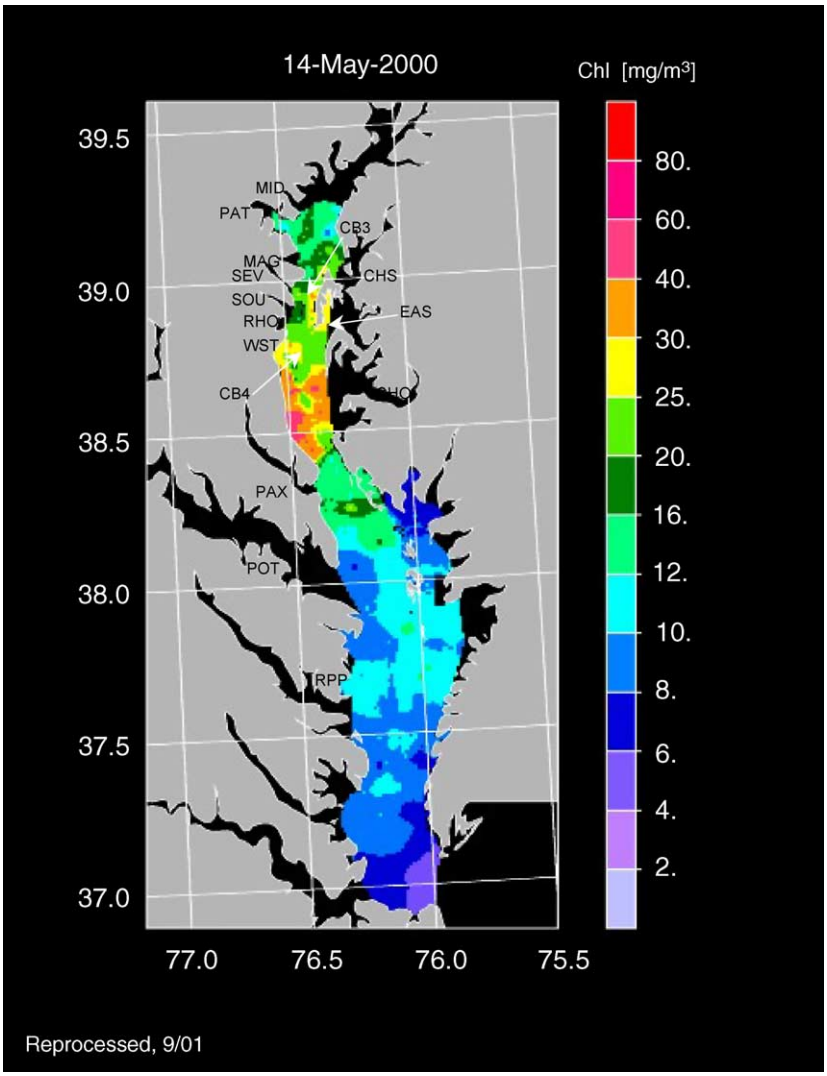

Fig. 1. Aircraft remote sensing retrieval of chlorophyll (Chl*a*) from the SeaWiFS Aircraft Simulator (SAS III), 14 May 2000 during the height of the *P. minimum* bloom in Chesapeake Bay. Highest chlorophyll areas were largely *P. minimum*, determined through field collections and pigment analyses (Adolf et al., in preparation). Segment locations for which water quality data and SAV impact data are available are shown by three-letter abbreviations, corresponding to first three letters of abbreviations given in Table 2: PAT: Patapsco River; MAG: Magothy River; SEV: Severn River; SOU: South River; RHD: Rhode River; WST: West River; PAX: Patuxent River; POT: Potomac River; CHS: Chester River; EAS: Eastern Bay; CHO: Choptank River; CB3: main stem mesohaline Chesapeake Bay 3; CB4: main stem mesohaline Chesapeake Bay 4. Image courtesy of the Chesapeake Bay Remote Sensing Program (http://www.cbrsp.org).

Using continuous monitoring of optical properties at a single location, Gallegos and Jordan (2002) documented the impact of the spring 2000 *P. minimum* bloom on light attenuation in the Rhode River, Maryland, a small tributary embayment on the western shore of Chesapeake Bay. The objective of this paper is to examine the extent to which this same bloom may have impacted light penetration and conditions for SAV growth in a wider array of sub-estuaries of the upper Chesapeake Bay. We examine the per cell and

per chlorophyll optical properties of water samples in which *P. minimum* was the overwhelmingly dominant phytoplankton species. Using these per cell properties, we construct a model of light penetration incorporating observed cell counts of *P. minimum* to predict the impact of the bloom on other locations from which *Prorocentrum* cell counts are available. We then compare predicted impacts with observed losses of SAV.

2. Optical properties and light attenuation

2.1. Diffuse attenuation coefficient

The decay of light intensity with depth, z, in the water is conveniently and empirically described by a negative exponential of the form,

$$E_d(\lambda, z) = E_d(\lambda, 0) \exp[-K_d(\lambda) z] \quad (1)$$

where $E_d(\lambda, z)$ is the cosine-corrected downwelling irradiance, $E_d(\lambda, 0)$ is the downwelling irradiance just below the water surface, and K_d is the diffuse attenuation coefficient. Both the irradiance and attenuation coefficient are functions of the wavelength of light, λ. Attenuation results from the combination of light absorption and scattering. Though more mechanistic models are available (Mobley, 1994), a simple and convenient expression relating diffuse attenuation coefficient, K_d, to the absorption and scattering coefficients is given by (Kirk, 1994)

$$K_d = \frac{1}{\mu_0} \sqrt{a^2 + g(\mu_0) ab} \quad (2)$$

where μ_0 is the cosine of the solar zenith angle refracted at the air–water interface, a the absorption coefficient, and b the scattering coefficient. The wavelength dependence of the absorption, scattering, and diffuse attenuation coefficients will be omitted for notational convenience except when needed.

The photosynthetic photon flux density, commonly referred to as photosynthetically active radiation (PAR, 400–700 nm) is defined as the quantum-weighted integral of $E_d(\lambda)$ over the visible wavelengths. A similar expression to Eq. (1) may be written for the depth-penetration of PAR, with the diffuse attenuation for PAR, K_d(PAR), replacing $K_d(\lambda)$, and surface-incident PAR replacing $E_d(\lambda, 0)$. Though the value of K_d(PAR) changes with depth in the water column due to wavelength-selective absorption, instrumentation for measurement of PAR is in widespread use in the monitoring and management communities, so that criteria for SAV survival have been established on the basis of the availability of PAR (Batiuk et al., 2000). Currently, the best estimates indicate that SAV in the mesohaline and polyhaline sections of Chesapeake Bay require about 22% of surface-incident PAR for survival. Thus, where other conditions are favorable (e.g., Koch, 2001), SAV appear to survive to depths where the dimensionless product $z \cdot K_d(\text{PAR}) \leq 1.5$ (Carter et al., 2000). For the purpose of this paper then, we desire to determine the impact of extraordinary blooms of *P. minimum* on the value of K_d(PAR).

2.2. Absorption coefficients, scattering coefficients, and water quality

Absorption and scattering coefficients depend on the amounts and kinds of materials dissolved and suspended in the water column. The absorption coefficient may be represented as the sum of contributions due to specific components, that is,

$$a_t = a_w + a_g + a_\phi + a_{p\text{-}\phi} \quad (3)$$

where a_t is the total absorption coefficient, and the subscripts, w, g, ϕ, and p-ϕ, refer, respectively, to water, colored dissolved organic matter (CDOM), phytoplankton pigments, and non-pigmented particulates (NPP).

The absorption spectrum of pure water is available as tabulated data (Pope and Fry, 1997). Absorption due to the other substances depends on the concentration of the relevant water quality parameter. We represent the spectral absorption due to water quality parameters as the product of a normalized absorption function representing the spectral shape, scaled by the absorption at a characteristic wavelength determined by proportionality with the water quality measurement. For example, we represent the absorption by phytoplankton as

$$a_\phi(\lambda) = \phi^*(676)[\text{Chl}a]\phi(\lambda) \quad (4)$$

where $\phi(\lambda) = a_\phi(\lambda)/a_\phi(676)$ is the normalized absorption spectrum of phytoplankton chlorophyll, Chl*a* is the concentration of chlorophyll a in mg m^{-3}, and

$\phi^*(676)$ is the specific-absorption of chlorophyll at 676 nm, determined by regression of $a_\phi(676)$ against Chl*a*. Similar expressions may be used to represent absorption by NPP and by CDOM, with additional simplifications that the normalized absorption spectra for NPP and CDOM may be expressed as negative exponentials with spectral slopes, s_p and s_g, respectively. Furthermore, the absorption by CDOM at the characteristic wavelength 440 nm is easily measured directly, and so is reported as absorption coefficient rather than scaled to some other water quality measurement (Cuthbert and del Giorgio, 1992). Thus, we have as a final expression for the total absorption spectrum,

$$a_t(\lambda) = a_w(\lambda) + a_g(440)\, e^{-s_g(\lambda-440)} + a^*_\phi(676)[\text{Chl}a]\phi(\lambda) + a^*_{p\text{-}\phi}(440) \times [\text{TSS}]\, e^{-s_p(\lambda-440)} \quad (5)$$

where TSS is the concentration of total suspended solids, and $a^*_{p\text{-}\phi}(440)$ is the specific-absorption coefficient of suspended solids at 440 nm.

Scattering is treated in a similar manner, except that water and dissolved substances do not contribute appreciably to scattering in estuaries, and it is not possible to physically separate phytoplankton from non-pigmented particulates in the measurement of scattering coefficients. In principle, we may write

$$b(\lambda) = b^*_\phi(555)[\text{Chl}a]b^n_\phi(\lambda) + b^*_{p\text{-}\phi}(555) \times [\text{TSS}]b^n_{p\text{-}\phi}(\lambda) \quad (6)$$

where $b^*_\phi(555)$ and $b^*_{p\text{-}\phi}(555)$ are specific-scattering coefficients at 555 nm and $b^n_\phi(\lambda)$ and $b^n_{p\text{-}\phi}(\lambda)$ are normalized scattering spectra for chlorophyll and NPP, respectively. In practice, however, there is no a priori guarantee that contributions from the different particle types will be distinguishable in mixed natural samples. Furthermore, the spectral shape of scattering is strongly dependent on particle-size distribution for NPP (Babin et al., 2003) and cell size and pigmentation for phytoplankton (Bricaud and Morel, 1986; Stramski et al., 2001). In this analysis, we attempt to isolate the effects of the Chl*a* term by restricting analysis to samples in which *Prorocentrum* was by far the dominant contributor to particulate matter.

3. Materials and methods

3.1. Optical measurements

Samples during the *Prorocentrum* blooms of 2000 and 2001 from the mouth of the Rhode River and from the Smithsonian pier about 3.8 km from the mouth were analyzed for inherent optical properties. In the laboratory, we measured absorption and beam attenuation coefficients of water samples using a WETLabs ac9 absorption and attenuation meter. Water was gravity-fed through the instrument at a flow rate of about 1.5 l min^{-1}, and data logged using the manufacturer's Wetview software. Absorption coefficients were corrected for sample temperature and salinity according to the manufacturer's instructions. Absorption coefficients were corrected for backscattering losses within the reflective tube (Kirk, 1992) as described by Gallegos and Neale (2002).

We measured absorption by CDOM on water filtered through a 0.2 μm pore-diameter polycarbonate membrane filter (Poretics) using 5 cm pathlength quartz cells in a Cary dual beam spectrophotometer. Measurements in absorption units (AU) were converted to in situ absorption coefficients, $a_g(\lambda)$, by multiplying by 2.303 [i.e., ln(10)] and dividing by the pathlength, 0.05 m.

We measured absorption by particulate matter, $a_p(\lambda)$, using the quantitative filter pad technique (Kishino et al., 1985). A volume of water was filtered onto a 25 mm glass fiber filter (Whatman GF/F, nominal pore diameter 0.7 μm) and frozen (−20 °C) for <4 weeks. For measurements, filters were thawed and re-wetted with 200 μl of filtered distilled water and placed next to the exit window of the sample beam of the Cary spectrophotometer. Absorbance was measured relative to a moistened (with distilled water) blank GF/F filter placed next to the exit window of the reference beam. Measured absorbances were converted into in situ particulate absorption coefficients multiplying by 2.303 and dividing by the geometric pathlength (=volume filtered/area of filter), and division by a pathlength amplification factor, $\beta = 1.5$ determined by comparison of filter pad measurements with solution absorption measured inside an integrating sphere (Babin and Stramski, 2002). Filters were extracted in methanol for 4 h at room temperature to extract phytoplankton pigments,

re-wetted, and scanned again in the Cary spectrophotometer to measure $a_{p\text{-}\phi}(\lambda)$. We then calculated $a_\phi(\lambda)$ as the difference, $a_\phi(\lambda) = a_p(\lambda) - a_{p\text{-}\phi}(\lambda)$.

3.2. Water quality measurements

Vertically integrated samples from stations in the Rhode River, Maryland were collected using a Labline (^{TM}) Teflon sampler that was slowly lowered and raised over the depth of the water column (1–3 m) to collect a vertically integrated sample. Water samples were transported to the laboratory where we measured optical properties and concentrations of optical water quality parameters. For determination of Chl*a*, whole-water samples were vacuum filtered onto GF/F filters in the lab, and stored frozen up to 4 weeks. Filters were thawed and extracted in 10 ml of 90% acetone overnight at 4 °C in the dark. Chlorophyll concentrations, uncorrected for phaeopigments, were calculated from spectrophotometric absorbance measurements by the equations of Jeffrey and Humphrey (1975).

Concentrations of total suspended solids in the Rhode River were determined on replicate subsamples from the weight gain of tared, pre-combusted (1 h at 510 °C) GF/F filters after filtration of a known volume and drying for 24 h at 110 °C. Filters were then combusted at 510 °C for 4 h and re-weighed to calculate fixed suspended solids.

Both of these methods were slightly different from those used for the Chesapeake Bay Program (CBP) Chl*a* and TSS data that are included in Table 4 for other segments. In CBP data, surface samples in Maryland were collected from 0.5 m below the surface using a pump, or 1.0 m below the surface in Virginia (RPPMH). CBP data also used Whatman GF/F filters with vacuum filtration in the field and similar extraction methods, but Chl*a* was corrected for phaeopigments, and total suspended solids filters were tared for dry weight but not pre-combusted (except from RPPMH), and they were dried at 105 C rather than 110 C.

3.3. Model calibration

To apply the model of diffuse attenuation coefficient for PAR, we need optical water quality concentrations (see below) and values for six constants: the spectral slope of absorption by CDOM, s_g, the spectral slope for absorption by NPP, s_p, specific-absorption coefficient for absorption by NPP, $a^*_{p\text{-}\phi}(440)$, specific-scattering coefficient by NPP, $b^*_{p\text{-}\phi}(555)$, specific-absorption coefficient of phytoplankton chlorophyll, $a^*_\phi(676)$, and the chlorophyll-specific scattering coefficient for *P. minimum*, $b^*_{p\text{-}\phi}(555)$, along with tabulated values for the absorption spectrum of pure water (Pope and Fry, 1997), the normalized absorption spectrum for phytoplankton chlorophyll, the normalized scattering spectrum for NPP, and the normalized scattering spectrum for *P. minimum*. Certain parameters tend to be relatively constant, or the variability has a minor effect on prediction of K_d(PAR), e.g., s_g and s_p. Others, e.g., $a^*_\phi(676)$, are rather variable, but not systematically so. Values used in this analysis are given in Table 1.

Experience has shown that the specific-absorption and -scattering coefficients of non-pigmented particulate matter need to be determined on a site-specific basis (Gallegos, 2001). This was done by a procedure that matched the model-calculated attenuation coefficient to observed median coefficient, using median

Table 1
Values of constants used in model of diffuse attenuation coefficient for photosynthetically active radiation (PAR) as a function of water quality measurements and density of *Prorocentrum minimum*

Parameter	Definition	Value	Units
s_g	Spectral slope of absorption by CDOM	0.0177	nm^{-1}
s_p	Spectral slope of absorption by NAP	0.009	nm^{-1}
$a^*_\phi(676)$	Specific-absorption coefficient for phytoplankton chlorophyll at 676 nm	0.026	$m^2\ mg^{-1}$
$a^*_{Pmin}(676)$	Specific-absorption coefficient for *Prorocentrum minimum* at 676 nm[a]	0.015	$m^2\ mg^{-1}$
$b^*_{Pmin}(555)$	Specific-scattering coefficient for *Prorocentrum minimum* at 555 nm[a]	0.092	$m^2\ mg^{-1}$
$a^*_{p\text{-}\phi}(440)$	Specific-absorption coefficient of NAP at 440 nm[b]	Variable	$m^2\ g^{-1}$
$b^*_{p\text{-}\phi}(555)$	Specific-scattering coefficient of NAP at 555 nm[b]	Variable	$m^2\ g^{-1}$

[a] Determined in this paper by analysis of samples dominated by *Prorocentrum minimum*.
[b] Determined on site-specific basis for selected segments by fit to median observed conditions.

Chl*a* and TSS concentrations in Chesapeake Bay segments of interest. Data from the Chesapeake Bay Water Quality Monitoring Program were selected for the months of April and May to match the timing of *Prorocentrum* blooms, and for Chl*a* less than 30 mg m^{-3} so that measurements of TSS would reflect mostly non-pigmented particulates. We additionally constrained the ratio of $a^*_{p\text{-}\phi}(440)$:$b^*_{p\text{-}\phi}(555)$ to 0.13, the average value in available samples from subestuaries around the mesohaline region of Chesapeake Bay (Gallegos unpublished). Data from available years (which varied amongst segments) prior to 2000 were used for estimation of specific-absorption and -scattering coefficients.

We tested this procedure using data from a station at the mouth of the Rhode River (about 2 km from CBP station WT8.3) where we have independent estimates of $a^*_{p\text{-}\phi}(440)$ and $b^*_{p\text{-}\phi}(555)$ made by direct measurements on water samples for comparison. The estimation procedure gave values of $a^*_{p\text{-}\phi}(440) = 0.071\ m^2\ g^{-1}$ and $b^*_{p\text{-}\phi}(555) = 0.529\ m^2\ g^{-1}$, compared with measured averages of $0.068\ m^2\ g^{-1}$ and $0.555\ m^2\ g^{-1}$, respectively.

Data on Chl*a* and TSS concentrations are available for a large array of additional sites from the Chesapeake Bay Water Quality Monitoring Program (CBP, http://www.chesapeakebay.net/data/). However, CDOM absorption is not measured by any water quality monitoring agencies in the CBP, and diffuse attenuation coefficient is not measured at many of the tributary stations, which complicates the calibration procedure. We have CDOM data from or near several segments of interest in this work, and assigned values to segments lacking CDOM data based on proximity to systems for which measurements were available. Using measured or assumed CDOM concentration, and measured median Chl*a* and TSS concentrations, we went through the calibration procedure to determine $a^*_{p\text{-}\phi}(440)$ and $b^*_{p\text{-}\phi}(555)$ for sites with measured K_d(PAR). For sites lacking measurements of K_d(PAR), we assigned values for $a^*_{p\text{-}\phi}(440)$ and $b^*_{p\text{-}\phi}(555)$ from a site with adequate measurements, again, based on proximity. Water quality values used and parameter values obtained by this procedure are given in Table 2.

3.4. SAV area, density, and depth data

SAV areas, bed densities, and bed depths used in this study were taken from the baywide aerial survey done once a year for each segment by the Virginia

Table 2
Values for median water quality concentrations, measured K_d(PAR), and calibrated specific-absorption and -scattering coefficients for non-algal particulate matter for selected mesohaline segments in upper Chesapeake Bay affected by the spring 2000 bloom of *Prorocentrum minimum*

Location	Abbreviation	CDOM (m^{-1})	CHL (mg m^{-3})	TSS (g m^{-3})	K_d(PAR) (m^{-1})	$a^*_{p\text{-}\phi}(440)$ ($m^2\ g^{-1}$)	$b^*_{p\text{-}\phi}(555)$ ($m^2\ g^{-1}$)
Middle River	MIDOH[a]	0.54	18.4	14.5	NA 1.86	PATMH	PATMH
Patapsco River	PATMH	0.47	13.6	12	1.58	0.103	0.770
Magothy River	MAGMH	SEVMH	11.6	12	NA 1.13	RHDMH	RHDMH
Severn River	SEVMH	0.36	12.7	11	NA 1.09	RHDMH	RHDMH
South River	SOUMH	RHDMH	22.8	15.5	NA 1.46	RHDMH	RHDMH
Rhode River	RHDMH	0.52	13.3	16	1.37	0.0606	0.452
West River	WSTMH	RHDMH	10.3	16	NA 1.33	RHDMH	RHDMH
Patuxent River	PAXMH	0.28	12.1	11	1.33	0.090	0.669
Eastern Bay	EASMH	CHO	8.1	10	NA 0.98	CHO	CHO
Potomac River	POTMH	PAXMH	10.5	11	1.38	0.097	0.725
Chester River	CHSMH	CHOMH2	7.6	12	1.00	0.053	0.398
Choptank River	CHOMH2	0.40	7.6	16	1.51	0.079	0.589
Chesapeake Bay	CB3MH	0.29	8.1	8.7	1.30	0.117	0.870
Chesapeake Bay	CB4MH	0.28	8.9	5.2	0.91	0.104	0.778
Rappahannock River	RPPMH[a]	0.37	8.0	16.0	1.89	0.111	0.827

Segments with numbers for all parameters are those for which all necessary data were available. Table entries with abbreviations refer to the segment used for an assumed value. Segments for which measurements of K_d(PAR) were not available (NA) required assumed values for the parameters $a^*_{p\text{-}\phi}(440)$ and $b^*_{p\text{-}\phi}(555)$, and the K_d(PAR) listed were calculated by the model. Chlorophyll (CHL), total suspended solids (TSS), and K_d(PAR) are medians of measurements during the months of April and May from the Chesapeake Bay Water Quality Monitoring Program.

[a] Middle and Rappahannock rivers were outside the bloom area to the north, and south, respectively.

Institute of Marine Science using data from 1996 to 2002. Photographs were taken at low tide near the peak of SAV biomass in each segment, usually in the summer. SAV area data were found at http://www.vims.edu/bio/sav/historical.html with 2001–2002 data added from http://www.vims.edu/bio/sav/sav02/tables/segarea_page.html. SAV density data were provided by Dave Wilcox at Virginia Institute of Marine Science, and SAV depth data were calculated by Howard Weinberg, University of Maryland Center for Environmental Science at the Chesapeake Bay Program Office. For comparing changes in density, we compared the percentage of the total SAV in each year that was in the highest density category in the VIMS survey, which represents visually estimated 70–100% cover. These dense beds tend to have the greatest habitat value and also to be more persistent than sparser beds. For comparing changes in bed depth, we examined the percentage of the mapped SAV in the shallowest category (0–1 m) as well as the percentage in the deepest category (>2 m).

The 1999 SAV survey was incomplete because Hurricane Floyd brought up to 12″ of rain in one day in mid-September that year, before the aerial photography was complete. In the segments that were not yet flown, the water was too turbid for photography for several days, and after the sediment settled out, most or all of the SAV that was present before Floyd was gone. The areas not surveyed within the area covered by this study were shaded pink in 1999 survey maps and included parts of Upper Central Chesapeake Bay and the Patapsco, Magothy and Severn rivers, although the portion of the Severn that was not flown was very small and has not had SAV mapped in it recently, thus we consider the Severn survey for 1999 to be complete. SAV survey data for 2001 were also incomplete because of airspace restrictions after the terrorist attacks, so they were not used in this comparison except in a few segments with complete data.

3.5. Additional sources of data

Data to determine the per cell chlorophyll concentration of *P. minimum* were taken from cruises on the Rhode River, Maryland at different times from the optical measurements. Data from *P. minimum* blooms in addition to spring 2000 were available due to the length of this sampling program. Samples were selected in which *P. minimum* was the highest ranking taxa in cell density, and that were collected in April or May in years known to be *Prorocentrum* bloom years (i.e., 1992, 2000, and 2001), from stations down-estuary from the influence of Muddy Creek, the local freshwater source to the Rhode River. The selection procedure yielded 46 samples from three stations among the 3 years.

Additional Chester River water quality data were collected by school-based volunteers, and were downloaded from http://www.qacps.k12.md.us/cms/sci/chesdata.htm. Monitors in this program use a salinity test kit made by LaMotte Inc. (Model POL-H, Code 7459) that uses chloride titration. Unpublished split sample data collected by one of the authors (PWB) in the Magothy River in 2002–2003 found that its results agreed well with salinity measurements using a conductivity meter, across the same range of salinities (0.3–18 ppt) encountered in the Chester River. Linear regression analysis between the paired measures of salinity showed that (Salin_Chloride) = 1.0239(Salin_Conductivity) + 0.3968, $R^2 = 0.973$, $N = 59$ pairs.

4. Results

4.1. Optical properties of Prorocentrum blooms

Large changes in the absorption and scattering spectra took place as the *Prorocentrum* bloom developed and declined in the Rhode River during spring 2000 (Fig. 2). The absorption due to phytoplankton at 676 nm, $a_\phi(676)$, increased from 0.92 m^{-1} on 20 April 2000 at the start of the bloom (Fig. 2a, squares) to >3 m^{-1} on 26 April (Fig. 2a, circles) corresponding to a Chl*a* increase from 60 to 172 mg m^{-3}. As Chl*a* declined to 11 mg m^{-3} on 16 May, total absorption remained near values at the onset of the bloom, but the absorption peak at 676 nm was lower than at bloom initiation (Fig. 2a, triangles).

The scattering spectrum at the onset of the bloom showed some inverse wavelength dependence and depression in the phytoplankton pigment absorption peaks at 443 and 676 nm, indicating a mix of small phytoplankton and non-pigmented particulate matter (Fig. 2b, squares). At the peak of the *Prorocentrum* bloom on 26 April, the scattering spectrum was flat,

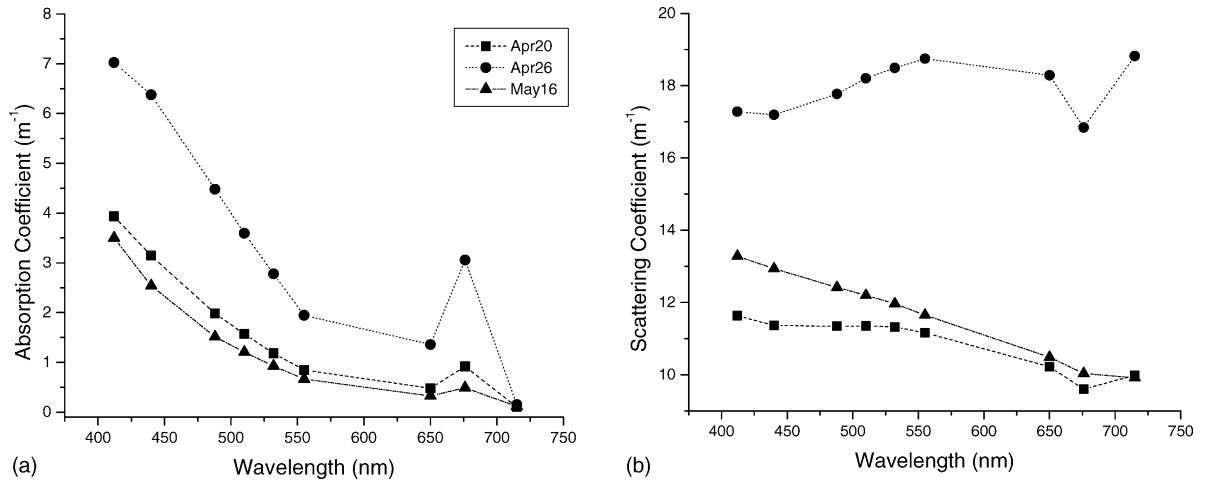

Fig. 2. (a) Spectrum of total-minus-water absorption coefficient at the onset (squares), peak (circles), and termination (triangles) of the bloom of *Prorocentrum minimum* in the Rhode River, Maryland, during the spring 2000. (b) As (a), for scattering coefficient.

with strong depression of scattering in the pigment absorption peaks, indicating dominance of the scattering by fairly large, monodisperse phytoplankton (Fig. 2b, circles), which we know in this case to be *P. minimum*. At the end of the bloom on 16 May, the scattering spectrum displayed strong inverse wavelength dependence and greatly reduced depression of scattering in the pigment absorption peaks (Fig. 2b, triangles), indicating dominance of scattering by small non-pigmented particulates which may have included a combination of lysed *Prorocentrum* cells (Gallegos and Jordan 2002 observed a spike in concentration of empty *Prorocentrum* thecae at the collapse of the bloom), bacteria (Morel and Ahn, 1990), and mineral particulates (Babin et al., 2003).

Due to the dominance of optical properties by *Prorocentrum* during the height of the bloom, we chose samples from this period, as well as some dates during April and May 2001 (when there was also a *Prorocentrum* bloom of lesser magnitude) for determination of normalized and specific-absorption and scattering spectra by *P. minimum*. The selection process yielded 24 samples for analysis of *Prorocentrum* optical properties.

The normalized absorption spectrum in the selected samples was less noisy than is typical of such measurements (e.g., Bricaud et al., 1995), due to the relative uniformity of species composition and growth conditions in the restricted sample set (Fig. 3a). Likewise, $a_\phi(676)$ was strongly correlated with Chl*a* (Fig. 3b). Linear regression gave a value of 0.016 $m^2\ mg^{-1}$ Chl*a* ($r^2 = 0.90$, $n = 24$) for the specific-absorption coefficient at 676 nm, $a^*_\phi(676)$.

All of the observed normalized scattering spectra exhibited some depression in the phytoplankton pigment absorption peaks at about 440 and 676 nm wavebands, as expected during a bloom heavily dominated by a single species, due to the resulting uniformity in the size distribution of the phytoplankton assemblage (Fig. 4a). Scattering coefficient at 555 nm was strongly correlated with Chl*a* in the selected subset of samples dominated by *Prorocentrum* (Fig. 4b). Linear regression gave a value of 0.092 $m^2\ mg^{-1}$ Chl*a* ($r^2 = 0.84$, $n = 24$) for the specific-scattering coefficient at 555 nm, $b^*_\phi(555)$.

Chl*a* was strongly correlated with *Prorocentrum* cell density in samples from spring blooms in the years 1992, 2000, and 2001 (Fig. 5). Linear regression gave a value of 4.4 pg Chl*a* $cell^{-1}$ ($r^2 = 0.94$, $n = 46$). Combined with the specific-absorption and –scattering coefficients estimated above, this regression (with appropriate conversion of units) provides a means of estimating the effect of *Prorocentrum* blooms on the absorption and scattering spectra at stations impacted by such blooms.

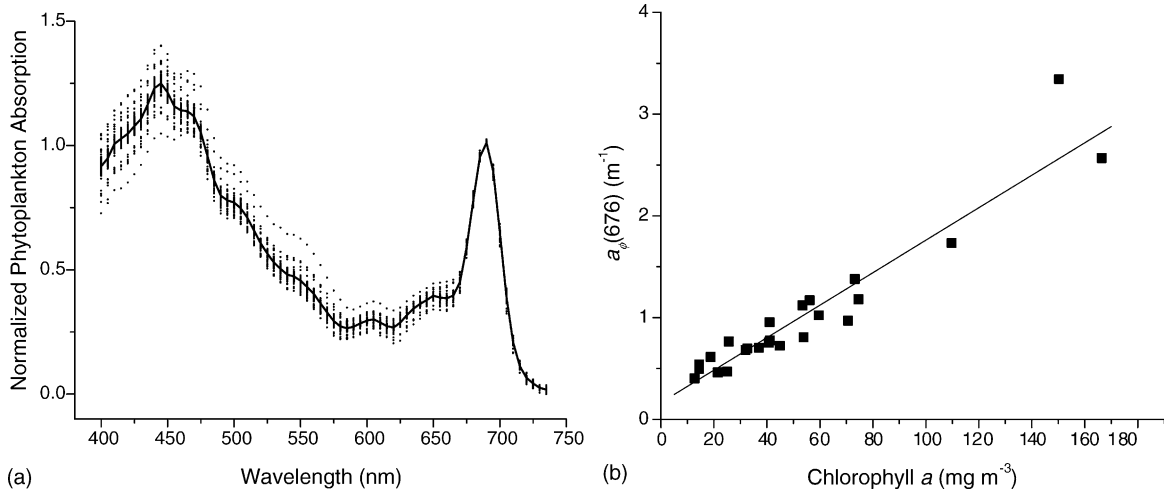

Fig. 3. (a) Normalized absorption spectrum for phytoplankton in samples dominated by *Prorocentrum minimum* during the spring blooms of 2000 and 2001 in the Rhode River, Maryland. Error bars are ±2 standard errors. Small dots are individual measurements. (b) Absorption by phytoplankton at 676 nm plotted against chlorophyll concentration in samples shown in (a). Line is fitted regression.

4.2. Modeling light attenuation due to *Prorocentrum* blooms

Diffuse attenuation coefficients predicted from interpolated cell counts compared favorably with measurements made in the Rhode River during the 2000 bloom (Fig. 6). We estimated uncertainty in the model prediction by conducting a Monte Carlo simulation, drawing optical water quality concentrations from random distributions, given in Table 3, to reflect the uncertainty in measurements (e.g., cell counts) and in quantities that were not directly measured. At the height of the bloom, uncertainty in modeled K_d(PAR) was governed almost entirely by potential errors in cell counts. One standard deviation of the simulated values

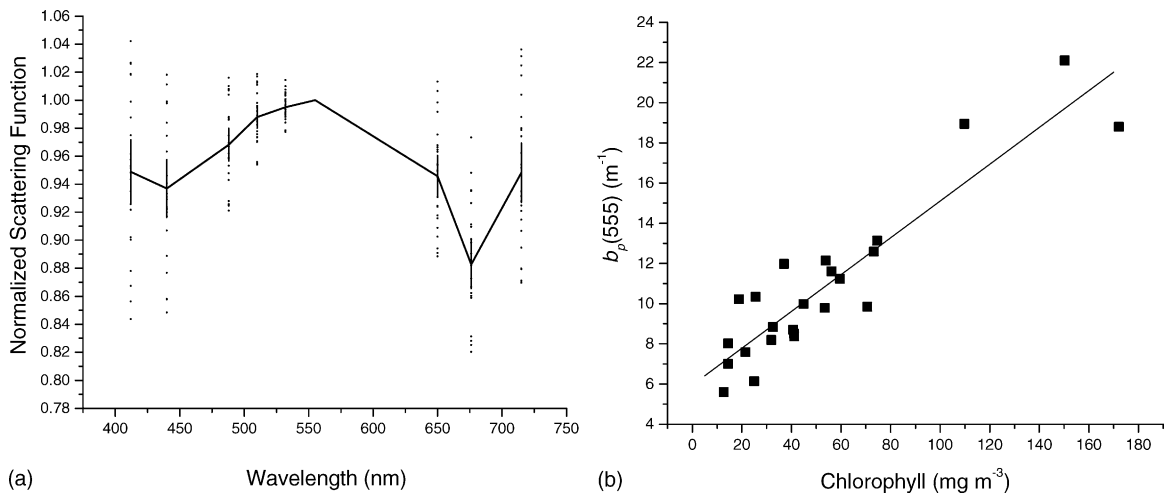

Fig. 4. (a) Normalized scattering spectrum for water samples dominated by *Prorocentrum minimum* during the spring blooms of 2000 and 2001 in the Rhode River, Maryland. Error bars are ±2 standard errors. Small dots are individual measurements. (b) Scattering by particulate matter at 555 nm plotted against chlorophyll concentration in samples shown in (a). Line is fitted regression.

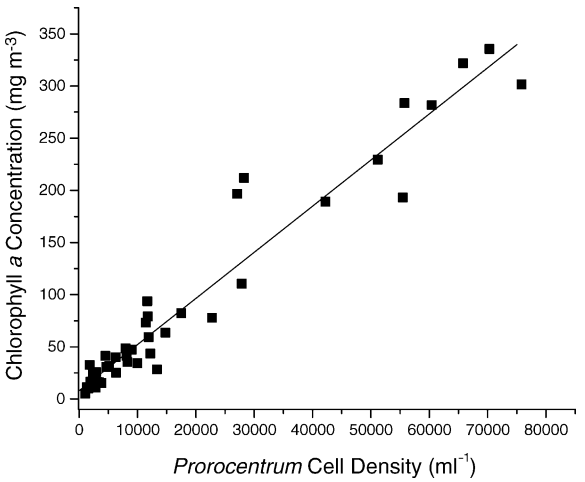

Fig. 5. Chlorophyll a concentration plotted against density of *Prorocentrum minimum* cells in samples known to represent *Prorocentrum* blooms. Line is fitted regression.

encompassed the observed value on the date simulated (Fig. 6).

In order to use data from the Chesapeake Bay Water Quality Monitoring Program to examine the impact of the spring 2000 *Prorocentrum* bloom on light

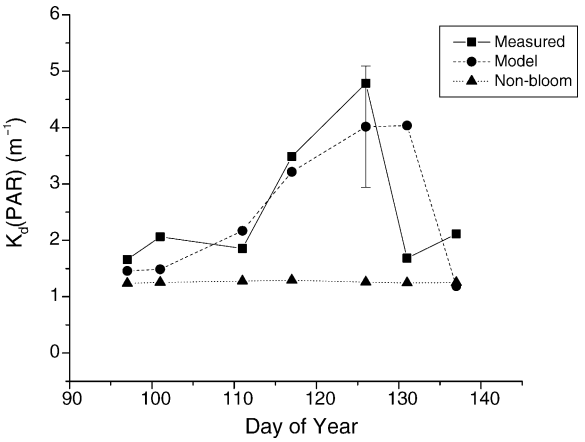

Fig. 6. Comparison of measured (squares) and modeled (circles) diffuse attenuation coefficients for photosynthetically active radiation [K_d(PAR)] during the spring 2000 bloom of *Prorocentrum minimum* in the Rhode River, Maryland. Model estimates were based on optical properties of *Prorocentrum minimum* cells and interpolated cell counts. Triangles: model estimates assuming no *Prorocentrum* cells and steady chlorophyll concentration of 20 mg m^{-3} (triangles). Error bars at day 126 model estimate are ±1 standard deviation determined by Monte Carlo simulation of the effects of uncertainty in input data (see Table 3).

Table 3
Distributions and parameters used to simulate uncertainty in model prediction of diffuse attenuation coefficient from water quality measurements and cell counts of *Prorocentrum minimum*

Water quality input	Distribution	Mean	S.D.	Units
CDOM	Normal	0.7	0.1	m^{-1}
Background CHL	Lognormal	2	1	mg m^{-3}
TSS	Normal	12	1.2	g m^{-3}
Cell density	Normal	50,000	10,000	cells ml^{-1}

S.D.: standard deviation.

attenuation in a variety of tributaries, it is desirable to first determine the adequacy of these data for this purpose. We therefore examined the data measured by the Chesapeake Bay Program (CBP) in the Rhode River in comparison with the more frequent data measured by the Smithsonian Environmental Research Center (SERC) (Fig. 7). The CBP sampling missed the timing of the peak Chl*a* concentration due to the bloom by about 8 days, and the maximal concentration measured by CBP was about 50% of that measured at the peak by SERC (Fig. 7a). Use of CBP Chl*a* data with the model of diffuse attenuation coefficient produced estimates that compared favorably with measurements prior to and during the bloom, but underestimated attenuation by about 30% at the termination of the bloom (Fig. 7b). Gallegos and Jordan (2002) found that an increase in absorption by non-pigmented particulate matter after the collapse of the bloom extended the impact of the bloom on light attenuation for an additional 2 weeks beyond that due to elevated Chl*a* alone. The underestimate at the end of the bloom in Fig. 7b is consistent with that process. Thus, we can expect that estimates of the impact of the *Prorocentrum* bloom on light attenuation using CBP data in other segments will be conservative, due to potential undersampling, and failure of Chl*a* or cell counts to gauge the full impact of the bloom.

4.3. Assessing the magnitude of the bloom

Aircraft remote sensing of surface Chl*a* in the main stem of Chesapeake Bay on 14 May 2000 (Fig. 1) indicated that Chl*a* exceeding 20 mg m^{-3} ranged from the Patapsco River to the mouth of the Patuxent River, peaking in the region of Calvert Cliffs (red region along the western shore). Variations in Chl*a* above 30 mg m^{-3} become difficult to resolve by remote sensing, due to the inherently non-linear relationship

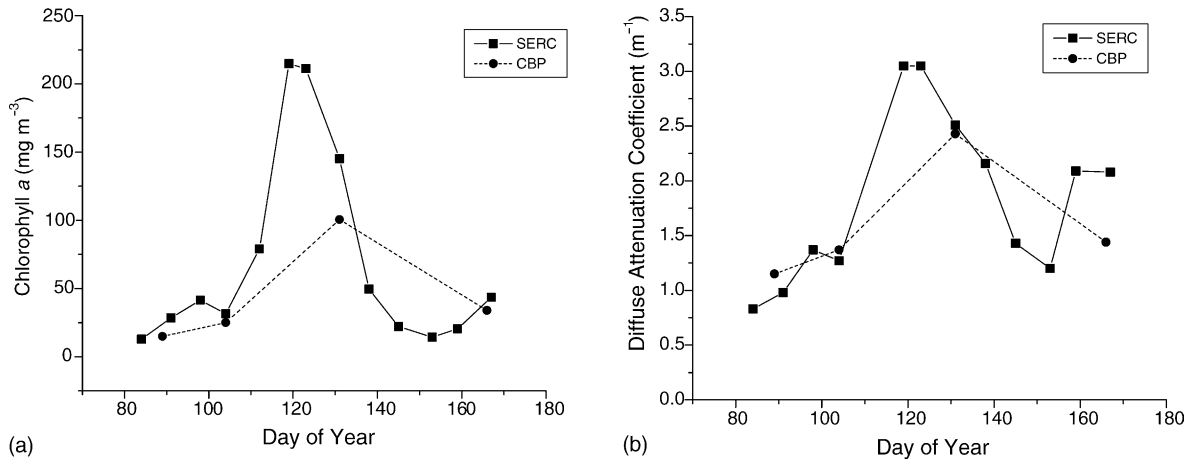

Fig. 7. (a) Time series of chlorophyll concentration measured (solid line and squares) at weekly intervals by the Smithsonian Environmental Research Center (SERC) and (dashed line and circles) at approximately monthly intervals by the Chesapeake Bay Program (CBP); (b) as (a) for diffuse attenuation coefficient. CBP values of attenuation coefficient were estimated using the optical model (see text).

between remote sensing reflectance and Chl*a*. Therefore, discrepancies between in situ measurements and aircraft measurements are to be expected (cf. Fig. 1, Table 4, CB4). Nevertheless, the main features of the north-to-south gradient of remotely sensed surface Chl*a* may be considered reliable.

Further comparison between in situ measurements (Table 4) and remotely sensed (Fig. 1) concentrations indicates that the tributaries generally experienced higher Chl*a* than the adjacent main stem, especially in cases such as the Potomac and Patuxent rivers. Given the problem of undersampling inherent in a

Table 4
Water quality concentrations used to calculate impact of the spring 2000 bloom of *Prorocentrum minimum* on light attenuation, and data to evaluate the extent of the bloom

Segment	Bloom peak chlorophyll (mg m^{-3})	Rank/# measured, % maximum	Bloom TSS (g m^{-3})	*P. minimum* density (ml^{-1})
MIDOH[a]	25.8	NA	10.3	NA
PATMH	38.3	12 (87) 38%	10.8	(8,699)
MAGMH	47.9	6 (56) 50%	8.4	(10,875)
SEVMH	261.7	3 (40) 66%	45.7	(59,468)
SOUMH	133.6	1 (38) 100%	19.3	(53,029)
RHDMH	100.6	2 (44) 74%	30.5	(22,852)
WSTMH	67.7	3 (39) 47%	22.8	(15,377)
PAXMH	128.1	1 (370) 100%	32.3	21,354
POTMH	433.6	1 (468) 100%	49.7	60,916
CHSMH	47.1	4 (105) 66%	21.3	(10,704)
EASMH	51.8	2 (77) 94%	12.7	(11,757)
CHOMH2	87.9	1 (82) 100%	23.0	9,590
CB3MH	71.2	7 (287) 48%	19.9	9,360
CB4MH	121.1	1 (739) 100%	25.7	9,332
RPPMH[a]	21.8	NA	15.6	NA

Cell densities in parentheses were calculated from measured chlorophyll using a conversion factor of 0.0044 (mg chlorophyll m^{-3}) (cells $ml^{-1})^{-1}$. The peak chlorophyll measured for the spring 2000 bloom is ranked, and percentage of maximum is given, relative to all surface observations (number of observations in parentheses) from the respective segments in the Chesapeake Bay Program water quality database for the months of April and May 1987–2002. Absorption by CDOM was not changed from value used to calculate K_d(PAR) under median conditions (see Table 2). TSS: total suspended solids; NA: not applicable.

[a] Segments MIDOH and RPPMH were, respectively, north and south of the bloom region.

monitoring program even as frequently as biweekly, it is difficult to determine the full extent of the *Prorocentrum* bloom in mesohaline Chesapeake Bay and tributaries. We list in Table 4 the peak Chl*a* measured by CBP for the sampling segments most impacted by the bloom. Surface Chl*a* measured during the spring 2000 bloom were the largest concentrations on record for the months of April–May 1987–2002 in five segments (Table 4). We know from Fig. 6a that the Chl*a* sampled by CBP for the Rhode River was about half the actual maximum. Based on historically observed concentrations, we suspect measured peak Chl*a* in the Chester, West, Patapsco, Magothy, and Little Choptank rivers and mesohaline mainstem segment CB3 were similarly underestimated. It is likely that the South, Potomac, Patuxent, and Choptank rivers, Eastern Bay, and the mainstem CB4 were sampled near peak concentrations.

4.4. Predicted impact of the bloom on light attenuation

Input parameters used to predict K_d(PAR) from water quality data are reported in Table 4. Data were taken from the date of the peak Chl*a* observed in April–May 2000. When available, cell counts of *P. minimum* were used as input; when counts were not available, all chlorophyll was assumed to be *P. minimum*, and absorption and scattering spectra were calculated as above. The diffuse attenuation coefficients predicted by the optical model agreed well with observed values for the segments in which measurements were available (Fig. 8a, inset).

Based on the available data, impacts of the mahogany tide on diffuse attenuation coefficient ranged from negligible (10–30% increase above the seasonal median in the Patapsco and Magothy rivers), to a greater than six-fold increase (Potomac River) (Fig. 8a). The attenuation coefficient was approximately doubled by the bloom in most other segments (Fig. 8a). At segments to the north (Middle River) and south (Rappahannock River) of the bloom area, attenuation coefficients were similar (Rappahannock) or even lower (Middle River) than the long-term seasonal median (Fig. 8a).

The depth of penetration of 22% of surface irradiance calculated from the attenuation coefficients (i.e., the presumed lower limit of SAV growth in mesohaline Chesapeake Bay) was greatly reduced by the mahogany tide. Under median (i.e., non-bloom) conditions, water quality in most of the examined segments would support growth of SAV to 1 m or below, at least based on conditions in April and May. The one exception, the Patapsco River, has had little or no SAV mapped in it since 1978. Due to the bloom, however, the average depth limit in segments impacted by the bloom was reduced to about 0.5 m (Fig. 8b). Segments north and south of the bloom region experienced some deepening (Middle River) or unchanged (Rappahannock River) depth of suitable light penetration (Fig. 8b).

4.5. Extent of SAV losses in 2000

In most segments, SAV losses in 2000 were assessed by comparing 2000 SAV areas to areas mapped in 1999 (Table 5). However, the 1999 survey was incomplete in some of the segments that had losses in 2000 (see Section 3), so the comparison had to be made to 1998 area in three segments.

Comparing 2000 SAV areas to 1998 and/or 1999 in segments that had some SAV in earlier years, SAV area declined in all of the segments adjacent to the Bay mainstem from the Patapsco River south to the mouth of the Potomac River on the Western Shore, and from the Chester River south to the Little Choptank River on the Eastern Shore (Table 5; see Fig. 1 for a segment locations). The largest losses in terms of area from 1999 to 2000 were in Eastern Bay (2005 ha), the mouth of the Choptank River (873 ha), and the lower Potomac River (418 ha); the SAV in all of these segments is dominated by widgeongrass (*Ruppia maritima*). The Lower Chester River lost 298 ha, but it had a more diverse mesohaline SAV community with several species. The Rhode River on the Western Shore and the Lower Choptank River on the Eastern Shore had no SAV mapped in 1998–2000 so they are not among the segments with declines.

We also examined changes in SAV density and depth over 1996–2000 to see if there were changes in these measures before and after the bloom. SAV beds that are stressed by low light availability might become less dense and/or shallower without changing in total mapped area, so these may be more sensitive indicators of SAV health than total area. However, since density and depth data are only available when there are mapped SAV, these results are more limited

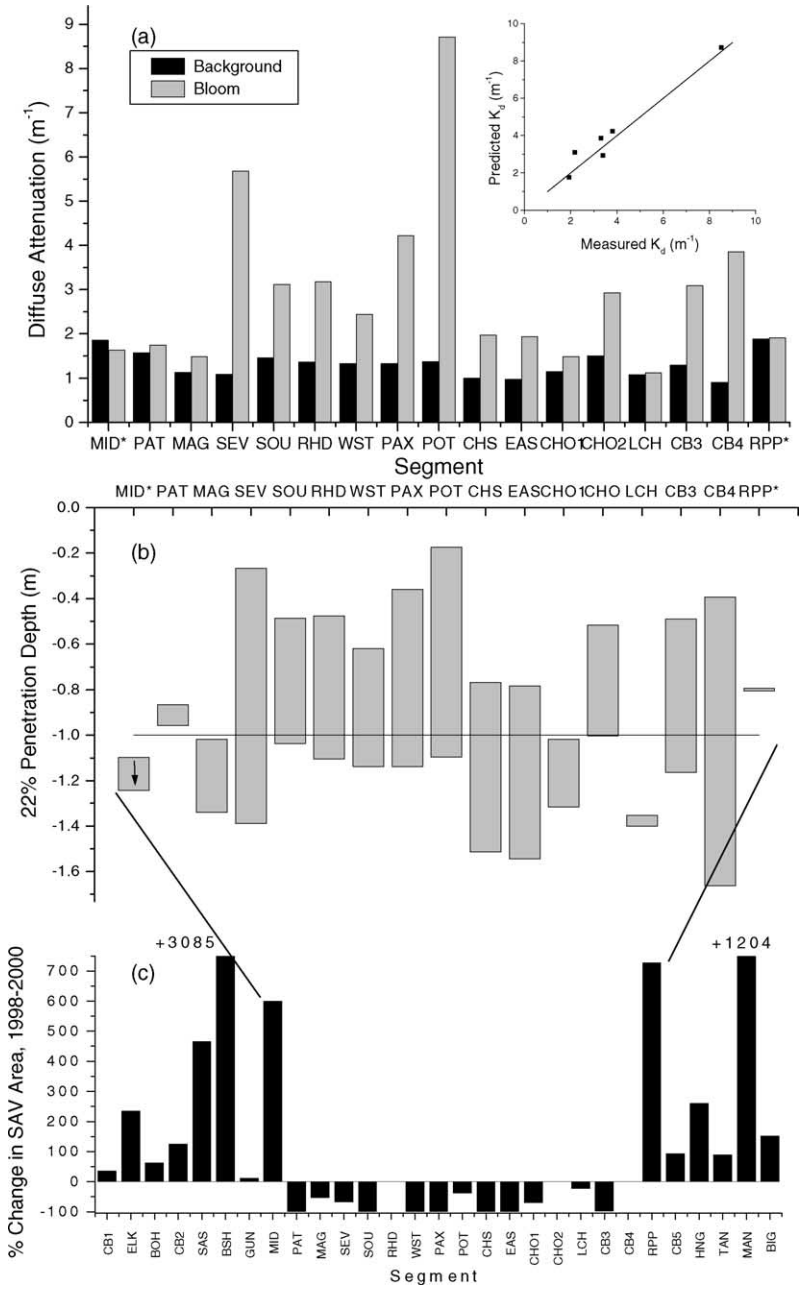

Fig. 8. (a) Predicted effect of *Prorocentrum minimum* bloom on diffuse attenuation coefficient for photosynthetically active radiation (gray bars) in relation to median value (black bars) for the spring time period for selected stations in tributaries of Chesapeake Bay (Maryland, USA). Inset shows predicted versus measured K_d(PAR) of stations for which measurements are available. Line of 1:1 agreement shown for reference. (b) Depth of penetration of 22% of surface irradiance. Bottom of bar is 22% penetration depth of median conditions, and upper end is the 22% penetration depth during the spring 2000 *Prorocentrum* bloom. Line at 1 m denotes Chesapeake Bay Program Tier II restoration goal. Segment names correspond to first three letters of those given in Table 2; locations given in Fig. 1. *Segments MID (Middle River) and RPP (Rappahannock River) were outside the bloom region to the north and south, respectively. Arrow for MID indicates increase in depth of light penetration; all other segments decreased. (c) Percent change in SAV area from 1998 to 2000, for segments in the bloom area and several segments to the north and south of it. Segments with no bar had no SAV in both years. See Table 5 for data used to calculate percent change and longer segment abbreviations.

Table 5
SAV area (ha) by CBP segment for segments in and adjacent to the bloom area

Segment	1996	1997	1998	1999	2000	2001	2002	% Change in area, 1998–2000	2002 as % of 1998 or 1999 peak
CB1TF[a]	2,146.8	2,490.0	2,310.1	2596.4 (pd)	3,143.5	3,230.5	3,735.7	36	
ELKOH[a]	43.7	67.4	206.1	323.2 (pd)	692.1	823.4	176.2	236	
BOHOH[a]	12.6	15.1	46.4	36.6	75.7	143.4	55.1	63	
CB2OH[a]	27.6	110.2	126.6	0.5	285.4	82.2 (pd)	203.3	125	
SASOH[a]	100.3	110.8	68.6	97.3	388.6	473.1	336.2	466	
BSHOH[a]	39.0	35.0	2.5	0 (pd)	78.7	1.19 (pd)	141.6	3,085	
GUNOH[a]	371.9	637.4	870.7	124.6 (pd)	984.6	0.0 (pd)	187.5	13	
MIDOH[a]	31.2	117.4	42.7	38.5	299.6	0.0 (pd)	254.8	601	
PATMH	2.3	1.9	5.9	0 (pd)	0.0	0.0 (pd)	3.2	−100	−45
MAGMH	37.2	53.5	80.0	26.4 (pd)	36.4	0.0 (pd)	84.5	−55	6
SEVMH	110.3	123.9	163.4	184.1 (pd[b])	51.9	48.5 (pd)	114.2	−68	−30
SOUMH	8.7	16.4	22.0	7.0	0.0	10.7 (pd)	14.4	−100	−35
RHDMH	0.0	0.0	0.0	0.0	0.0	0.0	0.0	0	
WSTMH	0.0	0.0	3.2	0.0	0.0	0.0	0.0	−100	−100
PAXMH	0.0	1.0	0.0	3.9	0.0	8.9	56.9	−100	1,359
POTMH	402.4	666.8	691.7	951.3	423.0	703.9	1,060.2	−39	53
CHSMH	311.8	424.8	477.9	297.7	0.0	83.2	82.9	−100	−83
CB3MH	364.5	370.8	308.3	2.8 (pd)	3.7	0.5 (pd)	38.3	−99	−88
EASMH	1,488.5	1,848.3	1,107.3	2,005.4	0.0	1,168.2	1,125.3	−100	−44
CHOMH1	2,343.7	2,792.6	2,283.3	1,533.6	680.7	2,128.5	2,665.8	−70	17
CHOMH2	0.0	1.8	0.0	0.0	0.0	60.0	62.5	0	
LCHMH	344.2	529.4	617.2	648.8	468.4	962.4	1,176.1	−24	81
CB4MH	0.0	20.3	0.0	9.8	0.0	45.4 (pd)	109.1	0	
RPPMH[a]	25.6	14.7	8.8	33.1	72.9	193.6	407.6	729	
CB5MH[a]	710.9	736.1	660.6	906.0	1,282.9	1,816.6	1,985.8	94	
HNGMH[a]	623.0	890.5	316.4	772.7	1,141.8	2,001.8	2,558.7	261	
TANMH[a]	4,461.7	3,825.6	2,675.7	4,299.3	5,087.7	5,388.5	6,082.6	90	
MANMH[a]	8.0	56.4	14.0	96.8	182.7	163.4	294.6	1,204	
BIGMH[a]	87.9	143.3	94.4	183.2	238.3	291.7	316.6	153	
CB1TF[a]	2,146.8	2,490.0	2,310.1	2596.4 (pd)	3,143.5	3,230.5	3,735.7	36	

Data from VIMS aerial survey; http://www.vims.edu/bio/sav/. In 1999 and 2001, (pd) = ''partial data'' (actual SAV area may have been higher). The causes of partial data were Tropical Storm Floyd (1999) and airspace restrictions (2001).

[a] Segments that were north and south of the bloom region are included here and in Fig. 8 for comparison purposes.

[b] SAV survey data for SEVMH in 1999 were considered complete because the area not surveyed was very small (see text).

than the data on SAV area. Only six of the 15 segments in the bloom area had mapped SAV in 2000, while two additional segments that had no mapped SAV in 2000 had enough data from other years to draw some conclusions about density and depth changes (Tables 6 and 7).

The percentage of the densest SAV declined in 2000 in all six segments with mapped SAV in 2000: the Magothy, Severn, Lower Potomac, mouth of the Choptank, Little Choptank, and Upper Central Chesapeake Bay (Table 6). The most dramatic decline was in the Severn River, which the highest percentage among these segments of mapped SAV in the densest category from 1997 to 1999, and this dropped to 0% in 2000 (Table 6). The Magothy and Lower Potomac rivers had a marked although smaller drop in the highest density category in 2000 (Table 6). Three of these six segments also had a decline in the highest density category in 1999 (Table 6). In two additional segments, the Lower Chester River and Eastern Bay, there was no SAV mapped in 2000 so density could not be calculated that year, but the percentage of mapped SAV in the highest density category in 1999, 2001 and 2002 was lower than in previous years. In Eastern Bay, the largest decline in the percentage in the highest density category occurred between 1997 and 1998, when it also had a 40% decline in SAV area (Tables 5 and 6).

Table 6
Percentage of the SAV mapped that was in each of four density categories, for segments in the bloom zone that had the most complete data

Segment and density	1997 (%)	1998 (%)	1999 (%)	2000 (%)	2001 (%)	2002 (%)
MAGMH 1	7.5	2.8		5.6		1.6
MAGMH 2	12.0	19.1		7.2		19.4
MAGMH 3	14.2	15.7		63.7		48.0
MAGMH 4	66.3	62.4		23.5		31.0
SEVMH 1	1.6	0.0	1.1	0.0		0.0
SEVMH 2	5.4	7.0	5.0	0.0		5.6
SEVMH 3	9.3	4.0	8.8	100.0		10.4
SEVMH 4	83.7	89.0	85.1	0.0		84.0
POTMH 1	4.7	5.4	15.5	28.9	8.5	12.6
POTMH 2	18.9	14.9	12.6	28.7	14.7	8.6
POTMH 3	10.9	9.0	14.3	22.3	22.7	28.3
POTMH 4	65.5	70.7	57.7	20.0	54.0	50.4
CHSMH 1	6.0	5.9	14.0		22.6	4.0
CHSMH 2	11.1	7.4	27.5		7.1	40.5
CHSMH 3	4.5	9.0	38.7		14.6	34.8
CHSMH 4	78.4	77.8	19.8		55.7	20.7
EASMH 1	9.9	15.3	10.9		10.0	1.8
EASMH 2	13.3	18.9	35.5		14.7	22.2
EASMH 3	17.3	29.5	19.7		34.3	42.1
EASMH 4	59.5	36.2	33.9		41.1	33.8
CHOMH1 1	7.3	3.7	3.5	17.8	10.3	4.8
CHOMH1 2	10.4	17.1	33.4	29.4	16.5	14.3
CHOMH1 3	9.1	12.3	33.3	10.8	37.4	46.8
CHOMH1 4	73.2	66.9	29.7	42.0	35.8	34.0
LCHMH 1	6.9	7.0	9.5	11.5	6.4	3.9
LCHMH 2	28.8	10.5	48.9	33.2	20.8	43.6
LCHMH 3	31.2	20.5	26.8	40.4	44.8	48.8
LCHMH 4	33.1	62.0	14.8	14.8	27.9	3.7
CB3MH 1	5.7	11.5		0.0		28.7
CB3MH 2	10.1	1.4		51.6		11.0
CB3MH 3	4.9	0.0		48.4		59.9
CB3MH 4	79.4	87.1		0.0		0.4

Density categories: 1 = 0–10% cover, 2 = 10–40% cover, 3 = 40–70% cover, 4 = 70–100% cover (visually estimated). Blanks in 1999 and 2001 mean incomplete data (SEVMH in 1999 was considered complete, see text), while blanks in 2000 mean no SAV was mapped (survey was complete).

The data on bed depth for these segments was less informative than the data on bed density, because the vast majority of the mapped SAV was already in the shallowest category (0–1 m) before the bloom occurred (Table 7). However, one segment (the Severn River) showed a change in the predicted direction (shallower SAV after the bloom). All of the segments in the bloom zone had at least 92% of their mapped SAV in the shallowest category before the bloom, and no more than 3% in the deepest category, except the Severn River (Table 7).

Comparing the distribution of segments with SAV losses in 2000 to the extent of the *Prorocentrum* bloom (see Section 4.3 above), we see that they occurred in the same areas. Segments north and south of this mid-Bay zone of declines all had SAV increases in 2000 (Fig. 8c). Note that Fig. 8c includes additional segments north and south of the bloom region to demonstrate the generality of these observations. Two of the larger increases in 2000 were in the Bush and Middle rivers on the Western Shore, just north of the area affected by *Prorocentrum*, and two other large increases were in the Lower Rappahannock and Manokin rivers south of the bloom area (Fig. 8c).

We also examined changes in SAV areas from 1998 to 1999 to see if the 2000 declines were part of a long-term decline in these segments. Of the segments that had SAV declines in 2000 that had complete 1999

Table 7
Percentage of SAV bed areas that were in the shallowest and deepest depth categories, for segments in the bloom zone that had the most complete data

Segment	1997 (%)		1998 (%)		1999 (%)		2000 (%)	
	% 0–1	% >2	% 0–1	% >2	% 0–1	% >2	% 0–1	% >2
MAGMH	98.1	0.0	97.5	0.0			100.0	0.0
SEVMH	81.5	4.8	79.8	5.5	77.2	6.0	90.4	1.9
POTMH	98.5	0.0	98.4	0.0	96.5	0.4	93.1	1.4
CHSMH	95.3	0.0	94.8	0.2	92.3	0.0		
EASMH	96.6	0.5	97.8	0.2	94.3	1.3		
CHOMH1	92.9	0.8	92.2	0.4	88.6	3.5	89.7	1.2
LCHMH	98.5	0.0	98.4	0.0	95.7	0.3	95.9	0.4
CB3MH	99.5	0.0	99.0	0.0			100.0	0.0

% 0–1 is the percentage of mapped SAV in water between 0–1 m deep MLLW, while % >2 is the percentage of mapped SAV in water over 2 m deep MLLW. Blanks mean incomplete data (1999) or no SAV was mapped (2000).

data, about half had increases from 1998 to 1999, and about half had decreases (Table 5). Those increasing in 1999 were the Severn River, lower Patuxent River (which went from 0 to 4 ha), lower Potomac River, Eastern Bay, and the Little Choptank River. Those decreasing in 1999 were the South and West rivers on the Western Shore, and the lower Chester River and the mouth of the Choptank River on the Eastern Shore. As noted above, SAV density declined in 1999 along with SAV area in the Lower Chester and the mouth of the Choptank, but density also declined in the Lower Potomac and Little Choptank, which had increases in SAV area in 1999. There were no marked changes in bed depth in the segments with declines in SAV area in 1999.

4.6. Possible effects on SAV of a smaller *Prorocentrum* bloom in 2001

There was also a spring *Prorocentrum* bloom in 2001, but it was of smaller magnitude than the 2000 bloom (http://mddnr.chesapeakebay.net/hab/news_5_23_01.cfm, maximum Chl*a* in Rhode River was 73 mg m^{-3}, Gallegos unpublished data, cf. Fig. 7a) and had a smaller spatial extent (http://www.cbrsp.org/cbrsp_toc_mb_chl_page.htm, cf. 24 May 2001). Whether it impeded SAV recovery in 2001 and 2002 (see next section) is hard to determine since several of the segments affected had incomplete SAV surveys in 2001, due to airspace restrictions after the 11 September 2001 terrorist attacks (Orth et al., 2002).

4.7. Recovery from the 2000 losses in 2002

The 2002 SAV survey results showed the largest increases compared to 2000 (58%) in the mid-Bay region, which starts at the Severn River and Eastern Bay and extends south to Tangier Sound. However, many of these same tributaries had declines in SAV area in 2000 compared to 1998 and/or 1999 (see above). The 2002 SAV areas were examined for these segments to see how many increased in 2002, and how many had reached or exceeded their 1998 and/or 1999 SAV areas, before the mahogany tide.

All of the segments in the zone that had SAV declines in 2000 had increases in 2002 (Table 5). The only segments with no SAV mapped in 2002 were the Rhode River, which has never had any mapped SAV since 1978, and the West River, which had 3 ha of SAV mapped in 1998 that was gone in 1999. One segment that had no SAV mapped in 1998–2000, the Lower Choptank River, had 63 ha mapped in 2002.

5. Discussion

5.1. Impacts of the spring 2000 *Prorocentrum* bloom on light availability for SAV

In water samples heavily dominated by *P. minimum*, optical properties were strongly related to Chl*a* (Figs. 3b and 4b), and Chl*a* was well correlated with *P. minimum* cell density (Fig. 5), permitting us to

construct a model of light attenuation based on *P. minimum* cell density or Chl*a*. For the Rhode River, model-estimated and measured attenuation coefficients during the peak of the bloom exceeded model-estimated coefficients based on median conditions for April and May by a factor of 3 for a period of 2–3 weeks (Fig. 6). Based on peak Chl*a* or cell densities of *P. minimum* measured biweekly, the spring 2000 bloom increased diffuse attenuation coefficients in other mesohaline segments of Chesapeake Bay by 10–600%, with concomitant reductions in the suitable habitat for SAV (Fig. 8).

The light attenuation model is not able to account for the increase in detrital absorption observed by Gallegos and Jordan (2002) at the termination of the bloom, except to the extent that the increase in detritus is captured in measurements of TSS. This increase in detrital absorption and scattering (which is not reflected in the measurement of Chl*a*) may account for the model underestimation of measured K_d(PAR) on the last sampling date shown in Fig. 6. Furthermore, the only water quality measurements available for application of the model are collected at mid-channel locations, generally removed from SAV growing sites. When specifically examined for the purpose of assessing SAV habitat requirements (Karrh, 2000), nearshore and mid-channel water quality measurements were found to give comparable results about 90% of the time, though nearshore and mid-channel measurements of TSS in the Magothy River frequently differed. For these reasons as well as problems of undersampling (Fig. 7), our model probably underestimates the full impact of the bloom on reduction in light availability in other mesohaline segments of Chesapeake Bay.

5.2. *To what extent can the 2000 decline in SAV be attributed to the Prorocentrum bloom?*

The fact that most of the segments with SAV declines in 2000 also had *Prorocentrum* blooms could be a coincidence, if those segments were already losing SAV due to other causes. However, as noted above, about half of the segments with declines over 1999–2000 had increases in 1998–1999, some of them quite large (the largest was the 900 ha increase in Eastern Bay, an 80% increase). Also, the fact that many of the segments with declines in 2000 had increases in SAV area in 2002 (see above) suggests that the declines in 2000 had relatively short-term causes in 1999 and/or 2000, rather than being part of a long-term SAV decline. Finally, the segment with one of the largest predicted decreases in water clarity during the bloom, the Severn River (Table 4 and Fig. 8a and b) was the only segment that had all three of the predicted effects of a reduction in water clarity on SAV: in 2000 it lost SAV area, SAV density, and SAV depth. SAV area and density in the Severn also showed recovery in 2002 after the bloom (depth data are not yet available for 2002). In the segment with the largest decrease in water clarity during the bloom, the Lower Potomac River (Table 4 and Fig. 8a and b), SAV was reduced in density during the bloom (Table 6) but not in depth (Table 7).

The SAV declines in 2000 also could have been completely or partially due to other causes. There was a baywide drought in 1998–1999, which essentially ended with Hurricane Floyd in mid-September 1999. These changes could have hurt SAV in three ways:

(1) Higher than normal salinity in 1999 could hurt lower salinity species;
(2) A rapid drop in salinity after Floyd could hurt some species; and
(3) Elevated turbidity after Floyd could hurt some species.

We examine each of these alternative causes in turn:

1. Of the segments that declined in SAV area 1999 based on complete surveys, high salinity could have been a cause of that decline in the Chester River. Salinity at Kent Narrows reached 18 ppt in September 2000 (based on Chester River Association data), which is beyond the upper salinity tolerance of most of the species that grew there except widgeongrass. High salinity in 1999 also could have caused a dieback of SAV in the Patapsco and Magothy rivers and Upper Central Chesapeake Bay, but they had only partial surveys in 1999. All of these segments have mesohaline SAV species that might die back during a drought. High salinity was probably not a factor in the other three rivers with SAV declines in 1999 (South and West rivers, and Mouth of the Choptank), because when they

have SAV they are dominated by widgeongrass that can tolerate salinities from 0 to 40 ppt (Stevenson and Confer, 1978). The very small SAV area mapped in the West River in 1998 (3 ha) has come and gone at least once before, so its disappearance was not remarkable, and the SAV area in the South River over 1996–1999 was only slightly higher, 7–22 ha (Table 5). The SAV area in the mouth of the Choptank River had been stable at 2300–2800 ha for three years before the decline in 1999 (Table 5), and its percentage in the densest SAV category also declined along with SAV area in 1999 (Table 6). However, the next segment to the north of it, Eastern Bay, had a large SAV area increase in 1999, after it had a large decrease in area in 1998 (Table 5). The adjacent segment to the south, the Little Choptank River, had a slight increase in SAV area in 1998 and 1999 (Table 5), although its percentage of SAV in the highest density category declined in 1999, along with that percentage in the Lower Potomac River (Table 6). Thus, it is not clear what caused the 1999 SAV decline in the mouth of the Choptank River.

2. The effects of a rapid drop in salinity on SAV are hard to evaluate because there are limited data on the size and speed of the drop in salinity, and there are no SAV survey data between when it occurred and the *Prorocentrum* bloom. Research has generally shown few effects of salinity changes on widgeongrass. The largest measured salinity drops after Floyd on the Chester River were 10.8 ppt at Gunston School and 6.0 ppt at Centreville Landing, but both stations are on a side tributary (the Corsica River), upriver of where SAV has been found in the Chester recently. Farther downriver on the Chester mainstem where SAV has grown recently, at Queenstown Creek and Kent Narrows, there was no drop in salinity after Floyd passed (based on Chester River Association data). Stevenson and Confer (1978) described widgeongrass as ‘‘unique among submerged aquatics’’ for its tolerance of variable salinity, but one study cited in Kantrud (1991) found that a 18 ppt drop in salinity over a few weeks killed widgeongrass in the Netherlands. However, other studies cited in Kantrud (1991) observed no ill effects on widgeongrass from more rapid changes in salinity of a similar magnitude. More recently, Chesnes (2002) found in experiments that widgeongrass sprigs remained healthy and viable after the salinity changed from 0 to 36 ppt every two days over a 24-day period. Thus, it is unlikely that any salinity drop after Floyd was a cause of the SAV dieback in 2000.
3. The possible effects of any elevated turbidity after Floyd are also hard to evaluate. It came before a network of devices that continuously monitor turbidity and other parameters were set up (see http://mddnr.chesapeakebay.net/eyesonthebay/index.cfm). Now that automated monitors are in place, it will be easier to evaluate the magnitude and duration of future turbidity pulses. Most of the measurements of Secchi depth before and after Floyd were not done often enough to document any drop. Relatively frequent data from the Chester River Association (twice a month) showed only one site with a drop in Secchi depth after Floyd, at Gunston School where it fell from 0.6 m on 6 September 1999 to 0.25 m on 19 September, but as noted above, this site is on a side tributary and is not close to any recent SAV in the Chester River. Kantrud (1991) cited several studies that reported disappearance of widgeongrass beds after a rapid increase in turbidity, and only one study (done in shallow water) that showed little or no impact of turbidity pulses. While rains from tropical storm Floyd were heavy in Baltimore-Annapolis region (300 mm), winds gusted to only about 90 km h^{-1} (NOAA National Climate Data Center), so that physical damage to SAV from Floyd is not likely.

One way to discriminate among possible causes is to examine their spatial extent relative to where the SAV declines occurred. The *Prorocentrum* bloom occurred in about the same area as the SAV declines, while the three other possible causes (listed above) affected larger areas. The first two of these, i.e., abnormally high salinity and a rapid salinity drop, affected the whole upper and middle regions of the Bay, where SAV species that cannot tolerate high salinity are found. The third other possible cause, high turbidity after Floyd, could have affected SAV baywide.

As noted above, most of the segments north and south of the bloom area had SAV increases in 2000, so alternative causes (2) and (3) are not very likely. However, many of the Upper Bay rivers where SAV

appeared to decline in 1999 due to high salinity had SAV increases in 2000 as salinity returned to more normal levels, including the Bush and Gunpowder rivers. As noted above, SAV declines in the Patapsco, Magothy and Chester rivers in 2000 may have been partially caused by alternative cause (1), high salinity in 1999, but it appears that the *Prorocentrum* bloom was also a factor in the decline. We argue that the SAV area in those rivers did not recover in 2000 as salinity returned to normal because the *Prorocentrum* bloom came at the start of the next growing season.

In conclusion, the strongest evidence for the *Prorocentrum* bloom causing SAV declines is that all of the segments that had blooms had SAV declines in 2000, while most of the segments outside the bloom area had SAV increases in 2000. The high salinity caused by the drought in 1999 may have been an additional cause of the 2000 SAV decline in a few segments that had less salinity tolerant species. These segments include the Patapsco, Magothy, and Chester rivers, and Upper Central Chesapeake Bay.

5.3. Likely impacts of the smaller spring 2001 *Prorocentrum* bloom on SAV area

Based on the available SAV survey data, it does not appear that this smaller and shorter bloom had a marked impact of SAV area. The one segment in the area affected that had complete 2001 SAV surveys, the Lower Chester River, had more SAV mapped in 2001 than in 2002, making it unlikely that the 2001 bloom had caused a further SAV dieback. Also, one of the segments in the 2001 bloom area, the Magothy River, had recovered to beyond its 1998 SAV area in 2002, again making it unlikely that the 2001 bloom had caused a further SAV dieback.

5.4. Implications for other estuaries

Our assessment of the impact of the *P. minimum* bloom on light availability for SAV in upper Chesapeake Bay was based on the light requirement of Chesapeake Bay SAV, and the effects of *P. minimum* on the inherent optical properties of the water. The SAV light requirements for Chesapeake Bay were determined from a literature review of field data and shading experiments, many of which were conducted at other locations and on species that do not occur in Chesapeake Bay (Carter et al., 2000). Thus, the Chesapeake-based requirement for 22% of surface irradiance at the maximum depth of colonization should have some measure of generality. For example, this Chesapeake light requirement was used successfully in a model for preliminary SAV restoration targeting in New England estuaries (Short et al., 2002).

However, converging lines of evidence examining epiphyte growth on SAV leaves suggested a requirement for 15% of surface irradiance at the leaf surface (Kemp et al., 2000). That is, plants in mesohaline and polyhaline Chesapeake Bay experience an average (but variable) additional attenuation of about 32% due to growth of epiphytes on leaf surfaces and co-accumulating particulate matter. Estuaries with consistently more or less epiphytic attenuation than this would require adjustments to the SAV light requirement.

Our estimates of light absorption and scattering by *P. minimum* cells were based on samples from the Rhode River, Maryland. While this is a potential source of site-specificity, our estimate of Chl*a* cell^{-1} for *P. minimum* is similar to that observed by Harding and Coats (1988) in samples from the main channel of Chesapeake Bay. We expect, therefore, that our estimate of the contribution of *P. minimum* to light absorption and scattering on a per cell basis should be reasonably robust. By formulating the model on the basis of inherent optical properties, the contribution of *Prorocentrum* to absorption and scattering can be added to that due to CDOM and non-algal particulates in any other system, but the latter two must be known. Thus, we have used an approach that is applicable anywhere, but to apply it elsewhere, site-specific studies to determine the local SAV light requirements are advisable, and determination of inherent optical properties (i.e., CDOM absorption and specific-absorption and -scattering coefficients of non-algal particulate matter) is essential.

6. Conclusions

P. minimum has been shown to be an organism with a high degree of physiological plasticity, so that its life history traits resonate with the seasonal progression of environmental forcing to produce recurring blooms of

extraordinary magnitude in mesohaline Chesapeake Bay and its tributaries. These life history traits include wide temperature and salinity tolerance (Tyler and Seliger, 1981), low light adaptation (Harding and Coats, 1988), utilization of multiple nitrogen sources (Fan et al., 2003), and switching to mixotrophy to survive times of low nutrient availability (Stoecker et al., 1997). These attributes allow the organism to utilize a physical circulation system that delivers seed populations to regions of high light and nutrient availability in late spring of years when the timing of the spring freshet coincides with optimal temperature for *Prorocentrum* growth. Tributary embayments, which afford much of the shallow water habitat required by submerged aquatic vegetation, are particularly vulnerable to these blooms. Moreover, the combination of events leading to the blooms occurs at a time that is particularly important to the life cycle of SAV (Moore et al., 1997). While there are uncertainties in attributing specific declines in SAV coverage to specific bloom events in conditions where other factors are never constant, the impacts of such extraordinary blooms on light penetration are unequivocal, as is the requirements of SAV for high light availability. Therefore, measures to reduce the magnitude and frequency of *P. minimum* blooms in Chesapeake Bay, which will undoubtedly entail reduction of anthropogenic nitrogen loading, must be viewed as an indispensable condition for restoration of conditions that will allow persistent, uninterrupted recovery of SAV to levels historically observed in mesohaline Chesapeake Bay.

Acknowledgements

The authors are grateful to Kevin Sellner for suggesting the idea for this paper and for many discussions of its content. Although the research described in this article has been funded in part by the Coastal Intensive Site Network (CISNet) program of the United States Environmental Protection Agency through grant R826943-01-0 to C.L.G., it has not been subjected to the Agency's required peer and policy review and therefore does not necessarily reflect the views of the Agency and no official endorsement should be inferred. Phytoplankton studies on the Rhode River, Maryland, were funded by the Smithsonian Environmental Sciences Program. We thank K. Yee and D. Sparks for assistance in the field and laboratory, S. Hedrick and S. Benson for collection and analysis of data from the Rhode River, D. Wilcox and H. Weinberg for providing SAV survey data, and M. Naylor and M. Trice for helpful suggestions. We thank Larry Harding for permission to use Fig. 1.

References

Adolf, J.E., Jordan, C.J., Miller, W.D., Mallonee, M.E., Harding Jr., L.W., in preparation. Phytoplankton floral composition and primary production in Chesapeake Bay.

Anderson, D.M., Glibert, P.M., Burkholder, J.M., 2002. Harmful algal blooms and eutrophication: nutrient sources, composition, and consequences. Estuaries 25, 704–726.

Babin, M., Stramski, D., 2002. Light absorption by aquatic particles in the near-infrared spectral region. Limnol. Oceanogr. 47, 911–915.

Babin, M., Morel, A., Fournier-Sicre, V., Fell, F., Stramski, D., 2003. Light scattering properties of marine particles in coastal and open ocean waters as related to the particle mass concentration. Limnol. Oceanogr. 48, 843–859.

Batiuk, R.A., Bergstrom, P., Kemp, W.M., Koch, E.W., Murray, L., Stevenson, J.C., Bartleson, R., Carter, V., Rybicki, N.B., Landwehr, J.M., Gallegos, C.L., Karrh, L., Naylor, M., Wilcox, D.J., Moore, K.A., Ailstock, S., Teichberg, M., 2000. Chesapeake Bay Submerged Aquatic Vegetation Water Quality and Habitat-Based Requirements and Restoration Targets: A Second Technical Synthesis. U.S. Environmental Protection Agency.

Bricaud, A., Morel, A., 1986. Light attenuation and scattering by phytoplanktonic cells: a theoretical modeling. Appl. Opt. 25, 571–580.

Bricaud, A., Babin, M., Morel, A., Claustre, H., 1995. Variability in the chlorophyll-specific absorption coefficients of natural phytoplankton: analysis and parameterization. J. Geophys. Res. 100, 13321–13332.

Bricelj, M.A., Lonsdale, D.J., 1997. *Aureococcus anophagefferens*: causes and ecological consequences of brown tides in U.S. and mid-Atlantic coastal waters. Limnol. Oceanogr. 42, 1023–1038.

Carter, V., Rybicki, N.B., Landwehr, J.M., Naylor, M., 2000. Light requirements for SAV survival and growth. Chesapeake Bay Submerged Aquatic Vegetation Water Quality and Habitat-Based Requirements and Restoration Targets: A Second Technical Synthesis, USEPA, Chesapeake Bay Program, pp. 4–15.

Chesnes, T.C., 2002. Responses of subtropical seagrasses to fluctuations in salinity within an experimental facility. PhD Dissertation, University of Florida, pp. 207.

Cuthbert, I.D., del Giorgio, P., 1992. Toward a standard method of measuring color in freshwater. Limnol. Oceanogr. 37, 1319–1326.

Fan, C., Glibert, P.M., Burkholder, J.M., 2003. Characterization of the affinity for nitrogen, uptake kinetics, and environmental relationships for *Prorocentrum minimum* in natural blooms and laboratory cultures. Harmful Algae 2, 283–299.

Gallegos, C.L., 2001. Calculating optical water quality targets to restore and protect submersed aquatic vegetation: overcoming problems in partitioning the diffuse attenuation coefficient for photosynthetically active radiation. Estuaries 24, 381–397.

Gallegos, C.L., Jordan, T.E., 2002. Impact of the Spring 2000 phytoplankton bloom in Chesapeake Bay on optical properties and light penetration in the Rhode River, Maryland. Estuaries 25, 508–518.

Gallegos, C.L., Jordan, T.E., Correll, D.L., 1992. Event-scale response of phytoplankton to watershed inputs in a subestuary: timing, magnitude, and location of phytoplankton blooms. Limnol. Oceanogr. 37, 813–828.

Gallegos, C.L., Jordan, T.E., Correll, D.L., 1997. Interannual variability in spring bloom timing and magnitude in the Rhode River, Maryland (USA): observations and modeling. Mar. Ecol. Prog. Ser. 154, 27–40.

Gallegos, C.L., Neale, P.J., 2002. Partitioning spectral absorption in case 2 waters: discrimination of dissolved and particulate components. Appl. Opt. 41, 4220–4233.

Harding Jr., L.W., Coats, D.W., 1988. Photosynthetic physiology of the dinoflagellate, *Prorocentrum mariae-lebouriae,* during its subpycnocline transport in Chesapeake Bay. J. Phycol. 24, 77–89.

Jeffrey, S.W., Humphrey, G.F., 1975. New spectrophotometric equations for determining chlorophyll *a*, *b*, *c1*, and *c2* in higher plants, algae and natural phytoplankton. Biochem. Physiol. Pfl. 167, 191–194.

Kantrud, H.A., 1991. Wigeongrass (*Ruppia maritima* L.): A Literature Review. U.S. Fish and Wildlife Service, Fish and Wildlife Research 10. Jamestown, ND: Northern Prairie Wildlife Research Center Home Page. http://www.npwrc.usgs.gov/resource/literatr/ruppia/ruppia.htm (Version 16JUL97).

Karrh, L., 2000. Comparing nearshore and midchannel water quality conditions. In: Chesapeake Bay Submerged Aquatic Vegetation Water Quality and Habitat-Based Requirements and Restoration targets: A Second Technical Synthesis. USEPA, Chesapeake Bay Program, pp. 131–156.

Kemp, W.M., Bartleson, R., Murray, L., 2000. Epiphyte contributions to light attenuation at the leaf surface. In: Batiuk, R.A., Bergstrom, P., Kemp, W.M., Koch, E.W., Murray, L., Stevenson, J.C., Bartleson, R., Carter, V., Rybicki, N.B., Landwehr, J.M., Gallegos, C.L., Karrh, L., Naylor, M., Wilcox, D.J., Moore, K.A., Ailstock, S., Teichberg, M. (Eds.), Chesapeake Bay submerged aquatic vegetation water quality and habitat-based requirements and restoration targets: A second technical synthesis. USEPA Chesapeake Bay Program, Annapolis, pp. 55–69.

Kirk, J.T.O., 1992. Monte Carlo modeling of the performance of a reflective tube absorption meter. Appl. Opt. 31, 6463–6468.

Kirk, J.T.O., 1994. Light and Photosynthesis in Aquatic Ecosystems, 2nd ed. Cambridge University Press, Cambridge.

Kishino, M., Takahashi, M., Okami, N., Ichimura, S., 1985. Estimation of the spectral absorption coefficients of phytoplankton in the sea. Bull. Mar. Sci. 37, 634–642.

Koch, E.W., 2001. Beyond light: physical, geological, and geochemical parameters as possible submersed aquatic vegetation habitat requirements. Estuaries 24, 1–17.

Loftus, M.E., Subba Rao, D.V., Seliger, H.H., 1972. Growth and dissipation of phytoplankton in Chesapeake Bay. I. Response to a large pulse of rainfall. Chesapeake Sci. 13, 282–299.

May, E.B., 1973. Extensive oxygen depletion in Mobile Bay, Alabama. Limnol. Oceanogr. 18, 353–366.

Mobley, C.D., 1994. Light and Water. Radiative Transfer in Natural Waters. Academic Press, New York.

Moore, K.A., Wetzel, R.L., Orth, R.J., 1997. Seasonal pulses of turbidity and their relations to eelgrass (*Zostera marina* L.) survival in an estuary. J. Exp. Mar. Biol. Ecol. 215, 115–134.

Morel, A., Ahn, Y.-H., 1990. Optical efficiency factors of free-living marine bacteria: Influence of bacterioplankton upon the optical properties and particulate organic carbon in oceanic waters. J. Mar. Res. 48, 145–175.

Orth, R.J., Wilcox, D.J., Nagey, L.S., Tillman, A.L., Whiting, J.R., 2002. 2001 Distribution of submerged aquatic vegetation in the Chesapeake Bay and coastal bays. VIMS Special Scientific Report Number 143.

Pope, R.M., Fry, E.S., 1997. Absorption spectrum (380–700) nm of pure water. II. Integrating cavity measurements. Appl. Opt. 36, 8710–8723.

Rensel, J.E., 1993. Severe blood hypoxia of Atlantic salmon (Salmo sala) exposed to the marine diatom *Chaetoceros concavicornis*. In: Smayda, T.J., Shimizu, Y. (Eds.), Toxic Phytoplankton Blooms in the Sea. Elsevier, New York, pp. 625–630.

Schubel, J.R., Pritchard, D.W., 1986. Responses of upper Chesapeake Bay to variations in discharge of the Susquehanna River. Estuaries 9, 236–249.

Sellner, K.G., Doucette, G.J., Kirkpatrick, G.J., 2003. Harmful algal blooms: causes, impacts, and detection. J. Ind. Microbiol. Biotechnol. 30, 383–406.

Short, F.T., Davis, R.C., Kopp, B.S., Short, C.A., Burdick, D.M., 2002. Site-selection model for optimal transplantation of eelgrass *Zostera marina* in the northeastern US. Mar. Ecol. Prog. Ser. 227, 253–267.

Stevenson, J.C., Confer, N.M., 1978. Summary of available information on Chesapeake Bay Submerged Aquatic Vegetation. U.S. Fish & Wildlife Service, FWS/OBS – 78/66.

Stoecker, D.K., Li, A., Coats, D.W., Gustafson, D.E., Nannen, M.K., 1997. Mixotrophy in the dinoflagellate *Prorocentrum minimum*. Mar. Ecol. Prog. Ser. 152, 1–12.

Stramski, D., Bricaud, A., Morel, A., 2001. Modeling the inherent optical properties of the ocean based on the detailed composition of the planktonic community. Appl. Opt. 40, 2929–2945.

Tyler, M.A., Seliger, H.H., 1978. Annual subsurface transport of a red tide dinoflagellate to its bloom area: water circulation patterns and organism distributions in the Chesapeake Bay. Limnol. Oceanogr. 23, 227–246.

Tyler, M.A., Seliger, H.H., 1981. Selection for a red tide organism: physiological responses to the physical environment. Limnol. Oceanogr. 26, 310–324.

Van Dolah, F.M., 2000. Marine algal toxins: origins, health effects, and their increased occurrence. Environ. Health Perspect. 108S, 133–141.